ScienSage

Journal of Advanced Scientific Research

Available online through http://www.sciensage.info/jasr

ISSN
0976-9595
Research Article

WOUND HEALING EFFICACY OF GREEN SYNTHESIZED SILVER NANOPARTICLES FROM *TECTONA GRANDIS* WOOD FLOUR EXTRACT IN WISTAR RATS

Pinki Dangi[1], Sandeep Choudhary[2]*, Digvijay Singh[3], OP Jangir[1]

[1]*Department of Biotechnology, Maharaj Vinayak Global University, Jaipur, Rajasthan, India*

[2]*School of Pharmaceutical Education & Research, Jamia Hamdard, Hamdard Nagar, Delhi, India*

[3]*Govt. Dungar College, Bikaner, Rajasthan, India*

**Corresponding author: pharmasan30@gmail.com*

ABSTRACT

Wound healing is a physiological process in which the tissue repairs itself after injury. Wound healing has attained a lot of attention as it is a complex phenomenon to maintain the integrity of skin after trauma. Stimulated wound closure without formation of scar or a faint scar is of great interest of dermatologist. Silver has been used to treat burns, wounds and infections in various forms. The tremendous developments in nanotechnology provide opportunities to modulates the metals into the nanosize and enhance their physical, chemical and physiological properties. Metallic silver in form of silver nanoparticles (AgNP) has been earlier reported to possess strong antimicrobial and antioxidant properties. Green synthesis is advancement in nanoparticle synthesis. In the present study, the effect of formulated nanoparticles using *Tectona Grandis wood floor* extract (green synthesized) was evaluated for ameliorating excision wounds in rats. AgNPs were synthesizes using an extract of T*ectona Grandis* wood floor extract as a reducing agent. The wound healing activity of AgNP in excision wound model in Wistar male rats was remarkable and equivalent to standard soframycin treatment. The results show amelioration of excision wounds using green synthesized AgNP could be a novel therapeutic way of improving wound healing in clinical practice.

Keywords: Wound Healing, Tectona Grandis, Wood flour Extract, Silver Nanoparticle

1. INTRODUCTION

Wound healing is an intricate process in which the tissue repairs itself after injury. Normally, in the skin, the epidermis and dermis exist in close steady-state equilibrium, forming a protective barrier against the external environment. On an injury, the protective barrier is broken and the normal (physiologic) process of wound healing immediately starts. The classic model of wound healing is divided into three or four sequential phases i.e., homeostasis, inflammation, proliferation and remodelling. Homeostasis involves the development of fibrin clot, and coagulation, followed by inflammation resulting in vasoconstriction or vasodilation, macrophage secretion and recruitment of other inflammatory cells. Subsequently, proliferation starts leading to angiogenesis, fibroplasia, epithelization and contraction, finally leading to tissue remodelling [1-3].

Within minutes post-injury, platelets aggregation take place at the injury site with fibrin to form a visible clot and controls the active bleeding.

The platelets secrete growth factors and inflammatory mediators to activate macrophages and fibroblasts. The fibrin product is indispensable to wound healing. Following, in the inflammatory phase, inflammatory cells (neutrophils and macrophages) remove injured tissue and provide protection from infection and release chemotactic and mitogenic factors. Later in the proliferative phase, fibroplasia takes place from the surrounding tissues onto the fibrin matrix to produce collagen, leading to epithelization, angiogenesis and contraction. Finally, the collagen molecules cross-link with already existing collagen there by increases the tensile strength of the scar. The tissue remodelling begins by the end of the second week and may continue for an indefinite period [1, 3, 4].

Pharmacological agents are used to accelerate the wound healing process. Silver has been used in various indications majorly in topical application, in form of metallic silver, silver nitrate, silver sulfadiazine etc [5]. Considering the potential of silver for wound healing application, its nanoparticles were formulated. Metallic

nanoparticles possess great interest due to their special chemical and physical characteristics. These characteristics create potential application in medicine, biotechnology, optics, microelectronics, catalysis, information storage etc [6, 7]. Nanoparticle synthesis usually involves chemical and physical methods, involving immense use of toxic chemicals and high temperature conditions. With a environment friendly perspective, to decrease the use of toxic chemicals and immense energy requirement, researchers have focused on bio-synthesis of nanoparticles [8]. Biological synthesis of nanoparticles utilizing microorganisms, enzyme and plant or plant extract, has been suggested as possible eco-friendly alternatives to chemical and physical methods [8, 9].

Plant and plant extracts act as reducing and capping agents in nanoparticle synthesis. Biosynthesis of nanoparticles by plant surpasses other biological methods by reducing the complicated process of maintaining cell culture [10-13]. The utilization of plant materials for the synthesis of nanoparticles is called as green synthesis as it does not involve any harmful chemicals, no organic solvent, with no harsh conditions, thus making it reliable, simple, energy efficient, cost-effective, self-sustaining and environment-friendly [10, 14, 15]. Water-soluble organics presented in the plant materials are mainly responsible for the reduction of silver ions to nanoparticles of silver [12, 16-19].

Silver nanoparticles (AgNPs) have been known to possess antimicrobial and antioxidant activity. Thus, there exists huge potential to use AgNPs for wound healing applications [12]. Green synthesis of AgNPs may also have significant applications in medical therapeutics.

Teak and its extracts from different parts have shown antioxidant activities, anti-inflammatory, antipyretic, analgesic, wound healing, free radical scavenging properties, diuretic and antibacterial properties [8, 20]. Some studies have been published showing the efficiency of teak –based biosynthesis of nanoparticles [8, 21].

Wood-flour--wood in a very fine particle form (consistency fairly equal to sand or sawdust) -is produced from the selected dry wood residue by several types of grinders and sized by mechanical or air screening methods. Reineke [22] states that the term wood flour "is applied somewhat loosely to wood reduced to finely divided particles approximating those of cereal flours in size, appearance, and texture."

2. MATERIAL AND METHOD

Silver nitrate, 99% (AgNO3) was obtained from Sigma-Aldrich, Germany. Phosphate-buffered saline (PBS), Methanol was purchased from Hi-Media Laboratories Pvt Ltd (Mumbai, India). Water used for the preparation of solutions was grade II water (Milli-Q grade from Elix 3, Millipore Corp., USA). All other chemicals used were of analytical grade and used as received without further purification.

2.1. Animals

Albino Wistar rats weighing between 220±20 g (age 8-10 weeks), were obtained from Govt. dungar college, animal house. The animals were acclatmized for one week; they were maintained in standard condition at room temperature (22±1°C), under a 12 h light/dark cycle. They had free access to water and food. The experimental protocol was approved by institutional animal ethics committee. The rats were divided into three groups namely control, standard treated, and AgNP treated, with minimum intergroup weight variation. (n=6)

2.2. Preparation of wood flour extract

T. Grandis wood was collected from the Aravali range of Rajasthan (India) and authenticated by a botanist in the Department of Botany, University of Rajasthan, Jaipur. The wood was grinded in fine powder/ wood flour. A 25 g of wood flour was boiled with 200 mL of deionized water for 25 minutes. The crude extract obtained, was filtered using Whatman No 1 filter paper (Whatman plc, Kent, UK).

2.3. Synthesis of AgNP

The AgNP were synthesized using method described elsewhere [8]. Briefly, 1mL of wood flour extract was added to 9 mL of 1mM aqueous $AgNO_3$ solution. The reaction mixture was allowed to stand at room temperature until the colorless solution converted into a reddish-brown color, indicating the formation of nanoparticles. The reduction of pure Ag ions was monitored by measuring the UV–Vis spectra of the solution, at different time points. A solution of biosynthesized AgNP was treated with NaCl solution (1% v/v) to remove un-reacted Ag ions. AgNP in the solution were then centrifuged at 12,000×g for 30 min, dried at 40 °C and maintained at 4 °C.

2.4. Characterization of AgNP

The reduction of pure Ag+ ions in presence of wood extract was monitored by measuring the UV-Vis spectrum at periodic intervals in a wavelength ranging from 350-500 nm. Morphological characterized was done by using Scanning Electron Microscope (FEI Quanta

400 ESEM FEG, Philips®, Netherlands). TEM was performed for observing the size and shape distribution of synthesized AgNP, by drying a drop of AgNP solution on carbon-coated TEM copper grids followed by measurements on a JEOL Model 1200 EX TEM operated at an accelerating voltage of 200 kV and analyzed with TECNAI G2 software. The particle distribution in the liquid was studied in a computerized controlled particle size analyzer (ZETAsizer Nanoseries, Malvern)

2.5. Wound healing activity

All assays were performed in accordance with institutional guidelines on ethical conduct in care and use of research animals according to CPCSEA (Committee for the Purpose of Control and Supervision of Experiments on Animals), New Delhi, India. Two studies, excision wound model and dead space wound model were carried out. Animals were randomly assigned to three groups according to different treatments: (i) control, no treatment received (ii) Standard, treated with (1% Soframycin) and (iii) AgNP treated.

2.6. Cutaneous wound healing assay on albino Wistar male rats

The excision wound was created on the rats under mild ether anesthesia. One excision wound of full thickness (1.5 cm diameter) was created on the dorsal side of the shaven rats (one per rat) using sterile surgical scissors. The wounds were then immediately traced onto a piece of sterile transparent graph sheet for knowing the exact size. The entire wound was left open. The wounds were immediately cleaned with sterile solution before the respective treatments were applied evenly in sufficient quantity to cover the wound. The treatment was repeated once in 24 h.

To determine the healing efficiency, the residual wound size was measured from the unclosed wound area after 4, 6, 9 and 14 days of post wounding [23, 24].

2.7. Wound contraction rate

The wound area (defined as the open skin surface) of each animal was measured on day 0 of surgery and also at days 3, 6, 9 and 14 of post-wounding. The data from each rat was calculated as the mean of triplicate measurements. Wound contraction rate was determined by taking the initial and final areas on to a transparent sheet. The wound contraction on a particular day were expressed as a percentage using the following formula [25].

$$\text{Wound Contraction on Day X (\%)} = \frac{\text{Wound area on Day 0 - Wound area on Day X}}{\text{Wound area on Day 0}} \times 100$$

Where X is day post wounding

2.8. Dead Space wound model

The animal were divided into three groups, under ether anesthesia, dead space wound were created by making a small incision on either side of dorsal paraverterberal surface of the rat, a sterilized cotton pellet (10mg) was carefully implanted, and the incision was sutured [26, 27]. After 14th day, the cotton pellet was excised under anastheia. After removing, cotton pellets wet weight was recorded. The cotton pellets were then dried in hot air oven at 70˚C for 24 hrs and the dry weight was taken, the granulation tissue thus, harvested was subjected to estimation of hydroxyproline, nitric oxide and glutathione.

2.9. Estimation of Nitric Oxide (NO)

The wet granular tissue was homogenised and supernatant was used for NO estimation. Equal volume of supernatant and griess reagent were mixed and incubated for 10 min at room temperature in dark, followed by spectrophometric determination at 548nm [27].

2.10. Estimation of Glutathione (GSH)

The above mentioned supernatant was also used for determining glutathione. To 1 ml of supernatant 0.2 ml of DTNB (dinitrobenzoic acid) was added. And further volume was made upto 3ml using 0.1 M phosphate buffer (pH 8). After incubation for 20 min the yellow colour change was measured at 412 nm [27].

2.11. Estimation of Hydroxyproline

After drying of cotton pellets recorded dry weight and cotton were hydrolyzed in 6N HCL at 130˚C for 4 hrs in sealed tubes. The hydrolysate neutralized to pH 7.0 and chloramine T was added for oxidation and the solution was kept for 20 minutes reaction. Reaction was terminated by the addition of 0.4 M perchloric acid and kept the solution for 5 minutes then added Ehrlich reagent to develop colour. The level of hydroxyproline was measured at 554 nm using autoanalyser [26].

2.12. Statical Analysis

The data were analysed by graph pad prism and result are expressed as mean±SEM. The significance of the difference in the response of treatment groups in comparison to the control was determined by one-way

analysis of variance (ANOVA) followed by tukeys test $p<0.001$, considered as highly significant, $p<0.05$ very significant, and $p<0.01$ was significant.

3. RESULTS

3.1. Preparation of wood flour extract

The wood flour extract obtained by 'decoction' was used for synthesis of AgNP by taking 1:9 ratio of wood flour and 1mM silver nitrate solution. The final nanopartilce were well dispersed solution that was subsequently confirmed by DLS. Aqueous solution of AgNP have brownish red colour, which may be due to surface Plasmon resonance.

3.2. Synthesis & Characterization of AgNP

Absorption spectra using UV spectrometer, of AgNP formed in the reaction media at 6 hrs has absorbance peak between 420-430 nm, broadening of peak indicated that the particles are poly dispersed (Fig. 1).

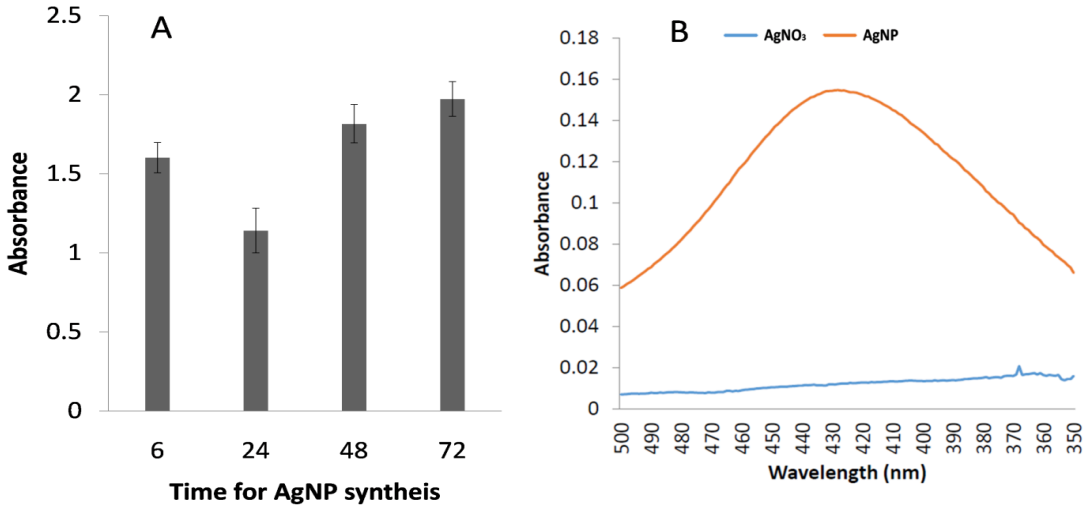

Figure 1: (A) The bar graph represents the absorption at λmax (426nm) against different time points. (B) The UV spectrum obtained from synthesized nanoparticles

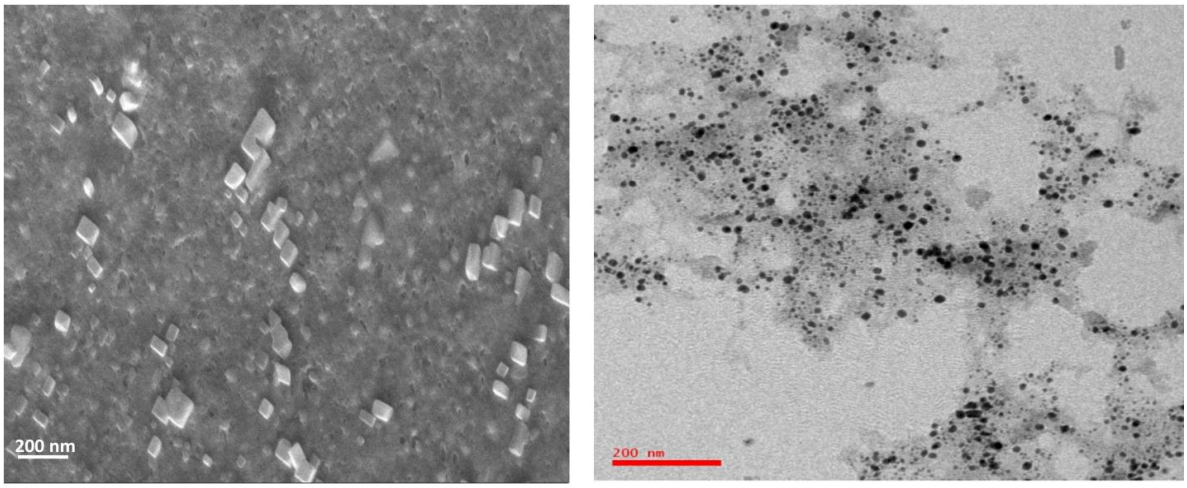

Figure 2: (a) AgNP at a resolution of 200 nm showing spherical and cubical nanoparticles using scanning electron Microscopy (SEM), (b) spherical AgNP using transmission electron Microscopy (TEM)

3.3. Scanning Electron Microscopy (SEM) & Transmission electron microscopy (TEM)

The images obtained from SEM analysis are shown in fig. 2(a). The shape of AgNP appears to be spherical to cubical with poly dispersed in nature. The size ranges from 50 nm to 200 nm.TEM analysis (Morgagni 268D) was performed for the prepared AgNP using. The TEM images obtained are presented in figure 2(b). The TEM images reveal the size of synthesized AgNP in the range of 30-50 nm which are spherical in shape.

3.4. DLS & Zeta potential analysis

DLS studies were performed on the prepared AgNP, Shows that the average diameter of the particles was found to be 190.8 nm with a polydispersity index of 0.261. Zeta potential analysis was performed on AgNP using ZETAsizer Nanoseries, Malvern instrument Nano Zs, indicate that the AgNP are small in size for which they are energetically very unstable. Therefore the particles undergo agglomeration/aggregation to stabilize themselves. So presence of potential charges on the surface of the nanoparticles makes them stable. Peak observed represents that the nanoparticles have charge of -3.68(mV), indicates that nanoparticles are very stable in nature.

3.5. Wound healing activity

3.5.1. Wound contraction rate

3.5.1.1. Wound closure rate

In the present investigation, the changes in macroscopic appearance, including the size variation of cutaneous excision wounds were monitored. The changes were visually assessed via a wound scoring system that scores the wound closure rate (WCR) and degree of inflammation. No adverse effect of topical treatment was noticed on body weight, general health or behavior of the rats. At three days post-wounding, the least healing was observed in the control group. Fig. 3 photographically represents wound healing with different treatments; Control, Standard drug, and AgNPs at 0, 4, 9 and 16 days post wounding. The WCR of control was observed to be 12%, 18% for standard treatment and 21% for AgNP, after 4 days post wounding.

The best healing, as evaluated by the closest apposition of the wound edges was clearly seen in the group treated with AgNPs. Fig. 3 shows wound closure rate (WCR) of control, standard and AgNP treated groups at different days post wounding.

At 9th day post-wounding, mild inflammation was commonly noticed in all the treated groups. The widest scars were seen in the control group with WCR of 44%. In the standard treatment group, narrow scars were seen in some, similar to group treated by the AgNP, with WCR of 56%. Visual signs of better healing were also observed in AgNP treatment with WCR of 60%.

At 16 days post-wounding, control showed partial healing with 67% WCR, followed by standard and AgNP treated with 95% WCR. The visual difference between AgNP and Standard treatment (WCR 94.3 & 95.5%, respectively) was non-significant. In this investigation, the wounds treated with AgNP healed faster than Control and was similar to standard treatment, which reveals that the topical application of AgNPs exhibited accelerated rate of wound healing.

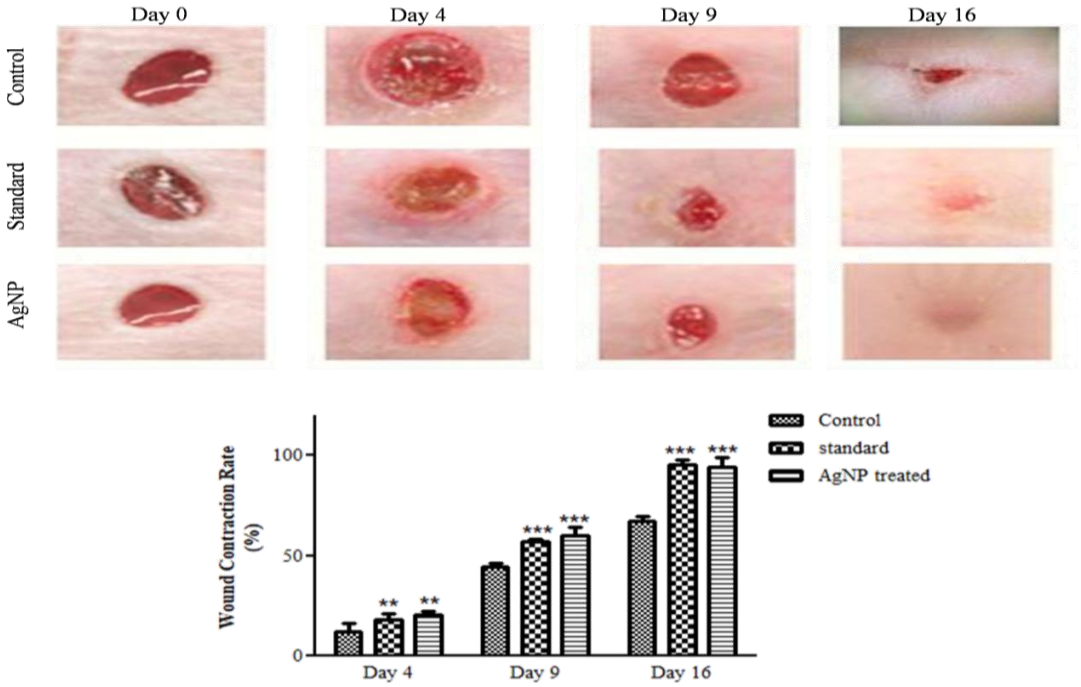

Fig. 3: Representaive images of rats showing wound contraction on different days post wound craetion, in excision wound model for all three group, i.e, control, standard treatment and AgNP treatment

*(N =6, mean ± s.d are represented, ***highly significant, ** very significant, *significant).*

3.5.2. Dead Space wound model

AgNP & Standard treatment caused a significant increase in wet weight mg /100 g body weight compared to control ($p<0.001$). Also both treatment significantly increased protein content compared to control, in granulation tissue by 18.3% and 17.4%, respectively ($p< 0.05$). Effect of AgNP was equivalent to standard with non significant differences.

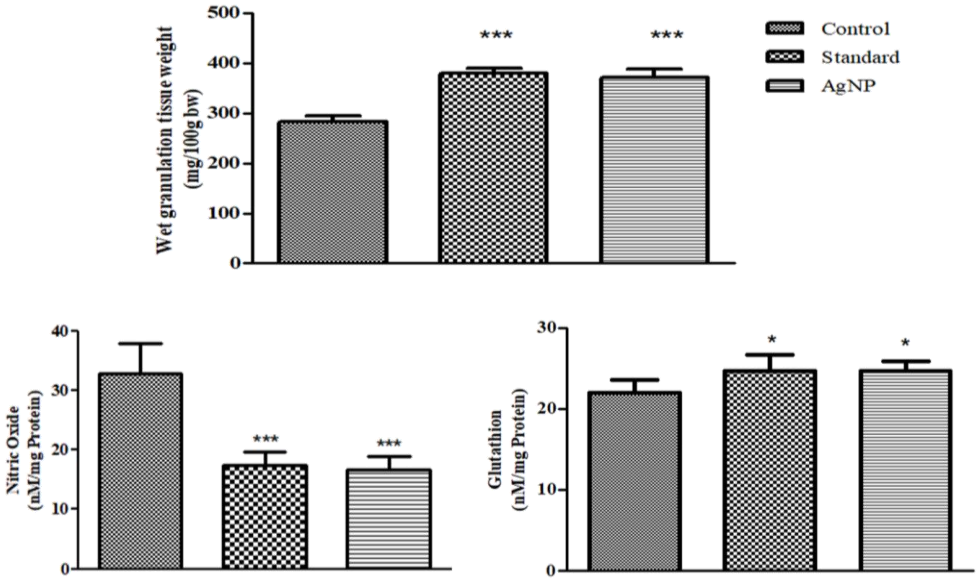

Fig. 4: The levels of tissue weight, Nitric oxide and glutathion

*(N =6, mean ± s.d are represented, ***highly significant, ** very significant, *significant)*

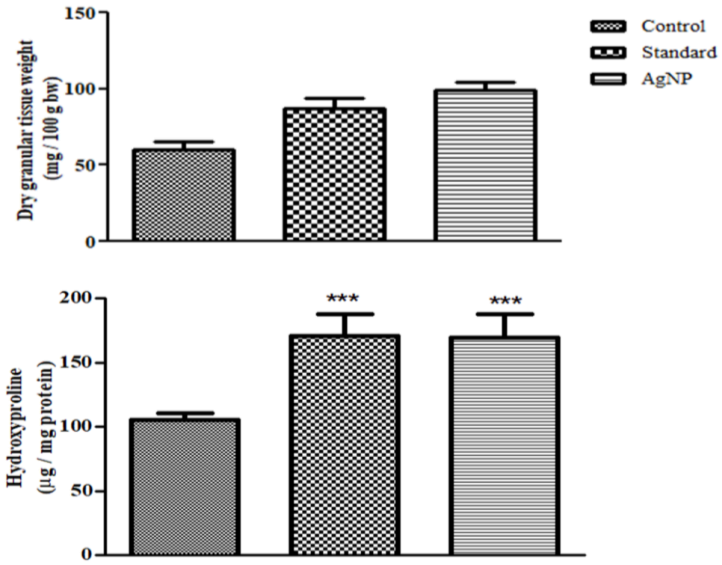

Fig. 5: The levels of dry granuation tissue weight and hydroxyproline in tissue.

*(N =6, mean ± s.d are represented, ***highly significant, ** very significant, *significant).*

3.5.3. Estimation of Nitric Oxide (NO)

The levels of NO (figure 4) in control significantly decreased on treatment with AgNP or standard drug, compared to control ($p<0.001$).

3.5.4. Estimation of Glutathion (GSH)

The levels of Glutathion(GSH, figure 4) level in treated group (AgNP & standard treatment) significantly increase compared to control groups ($p<0.05$).

3.5.5. Estimation of Hydroxyproline

The levels of hydroxyproline in dry granular tissue (fig. 5) were significantly increased compared to control for both AgNP and standard treatment ($p<0.001$).

4. DISCUSSION

Green synthesis of metal nanoparticle involves the use of biological reducing agents, producing eco-friendly and

pollution-free metal nanoparticles. Green synthesis has recently gained popularity in research due to their cost effective and simple method of preparation. In addition the biologically-mediated synthesis is dependable and environmentally friendly approaches preventing from the hazardous effects of chemical mediated processes.

The green synthesis utilizes the potent active principals of plant extract e.g., amino acids, proteins, or secondary metabolites as flavanoids, terpenoids, alkaloids etc. for the prevention of particle aggregation. Thus, Biological methods seem to provide controlled particle size and shape, which is an important factor for various biomedical applications [28].

In the present study, Ag-NPs were synthesized using wood flour extract from *T. Grandis*, thus revealing that *T. grandis* wood flour extracts can be used as an effective stabilizing reducing and capping agent for the synthesis of AgNP. The AgNP were found to be polydisperesed with spherical and cubical shape with size ranging from 30-190 nm. The charge on Nanoparticles helps to get stabilized nanoparticles. In previous communication, AgNP have been shown to possess antifungal and antibacterial activity (against both gram positive and gram negative bacteria). Additionally, the AgNP as well as the aqueous plant extract was found to have good antioxidant capacity and free radical scavenging assay [8].

Wound healing is an intricate process in which the tissue repairs itself after injury due to defense mechanism of body's immune system but it take more time to heal the untreated wound compared to drug treated wound. In excision wound model AgNP treated group showed more wound contraction and enhanced epithelization as compared to normal and treated group. In dead space model there was also significant increase in hydroxyproline which is responsible for the collagen synthesis. AgNP and standard treated group showed more dry granulation weight indicate higher protein content. Also, the levels of NO were decreased, that indicates a free radical scavenging mechanism of AgNP action for wound healing. In addition, it also boosts the internal antioxidant defense system, shown by increase in glutathione levels.

Therefore on the basis of above results we can say that AgNP promotes healing of wound, by increasing rate of collagen synthesis, period of epithelization, wound contraction in rats and boosting antioxidant status of the tissue.

A therapeutic agent selected for the treatment of wounds should potentially improve one or more phases of healing without producing injurious side effects. Technologies that can facilitate wound healing are in demand; advances in nanotechnology have resulted in the ability to produce pure silver as nanoparticles. It is therefore, hypothesized that AgNPs could improve the healing of incision wounds initially on the basis of the known antimicrobial and antioxidant properties. Epithelialization of wound in AgNP treated animals was completed in 16 days after the excision wound, while only partial epithelialization was observed in control rats. The collagen concentration in the epithelialized tissue indicates the potency of wound healing which gets accelerated during the process of repair and regeneration [24, 29]. These results also indicate significant increase in collagen deposition within the granulation tissue in experimental groups possibly due to increase in synthesis of collagen/ protein and could be correlated with the effectiveness of wound healing.

The results here show that application of AgNP could greatly increase the collagen deposition in the wound at day 16 post wounding compared to control, which might be because of its high anti-oxidant activity, which is in accordance with previous report [8]. With the most impressive effect in antimicrobial and many other broad-spectrum biomedical and healthcare, AgNPs in real applications is still a controversial issue.

5. CONCLUSION

Formulations using green synthesized AgNPs have been used to demonstrate effectiveness in wound healing process in Wistar rat model. The results show that topical application of green synthesized AgNPs on open skin wound induced significant granulation tissue formation, collagen deposition, re-epithelialization and accelerated wound closure compared to control. Thus, it could be clearly demonstrated that topical application of green synthesized AgNPs paves a simple and reliable method of wound healing.

6. REFERENCES

1. Wang P-H, Huang B-S, Horng H-C, Yeh C-C, Chen Y-J. *J Chinese Med Assoc.*, 2018; **81(2):**94-101.
2. Agrawal P, Soni S, Mittal G, Bhatnagar A. *Int J Low Extrem Wounds*, 2014; **13(3):**180-190.
3. Eming SA, Martin P, Tomic-Canic M, et al. *Sci Transl Med.*, 2014; **6(265):**265sr6.
4. Kryczka J, Boncela J. Leukocytes: *Mediators Inflamm*, 2015;**1-10.**
5. Rai M, Yadav A, Gade A. *Biotechnol Adv.*, 2009; **27(1):**76-83.

6. Zhang H-M, Zhang Y. *J Pineal Res.*, 2014; **57(2):**131-146.
7. Rahi DK, Parmar AS, Tiwari V. *Int J Pharm Pharm Sci.*, 2014; **6(11):**160-166.
8. Dangi P, Jangir O. *Asian J Pharm Clin Res.*, 2019; **12(1):**257.
9. Bhandari M, Raj S. *Int J Pharm Pharm Sci.*, 2017; **9(4):**10-26.
10. Kaler A, Jain S, Banerjee UC. *Biomed Res Int.*, 2013; **2013:**1-8.
11. Singh G, Babele PK, Shahi SK, Sinha RP, Tyagi MB, Kumar A. *J Microbiol Biotechnol.*, 2014; **24(10):**1354-1367.
12. M GS, Saha S, John N, et al. *Int J Pharm Appl.*, 2013; **4(1):**19-28.
13. Narayanan KB, Sakthivel N. *Adv Colloid Interface Sci.*, 2010; **156(1-2):**1-13.
14. Atta A, Al-Lohedan H, Ezzat A. *Molecules*, 2014; **19(5):**6737-6753.
15. Anbarasu A, Karnan P, Deepa N, Usha R. *Int J Curr Pharm Res.*, 2010; **10(3):**15-20.
16. Devadiga A, Shetty bullet K Vidya, Saidutta bullet MB, Shetty KV, Saidutta MB. *Int Nano Lett.*, 2015; **5(4):**205-214.
17. Okafor F, Janen A, Kukhtareva T, Edwards V, Curley M. *Int J Environ Res Public Health*, 2013; **10(10):**5221-5238.
18. Singh K, Panghal M, Kadyan S, Chaudhary U, Yadav JP. *J Nanobiotechnolog,* 2014; **12(1):**40.
19. He Y, Du Z, Lv H, et al. *Int J Nanomedicine*, 2013; **8:**1809-1815.
20. Vyas P, Yadav DK, Khandelwal P. *Nat Prod Res.*, 2018:1-17.
21. Devadiga A, Shetty KV, Saidutta MB. *Int Nano Lett.* 2015; **5(4):**205-214.
22. Reineke LH. *Wood Flour.*; 1961. https://ir.library.oregonstate.edu/concern/defaults/tb09j9991. Accessed March 28, 2018.
23. Lei Z-Y, Chen J-J, Cao Z-J, Ao M-Z, Yu L-J. *J Ethnopharmacol.*, 2019; **228:**156-163.
24. Naraginti S, Kumari PL, Das RK, Sivakumar A, Patil SH, Andhalkar VV. *Mater Sci Eng C.*, 2016; **62:**293-300.
25. Nagar HK, Srivastava AK, Srivastava R, Kurmi ML, Chandel HS, Ranawat MS. *J Pharm.*, 2016; **2016:**1-8.
26. Shenoy RR, Sudheendra AT, Nayak PG, Paul P, Kutty NG, Rao CM. *J Ethnopharmacol.*, 2011; **133(2):**608-612.
27. Murthy S, Gautam MK, Goel S, Purohit V, Sharma H, Goel RK. *Biomed Res Int.*, 2013; **2013:**972028.
28. Zhang X-F, Liu Z-G, Shen W, Gurunathan S. *Int J Mol Sci.*, 2016;17(9).
29. Özay Y, Güzel S, Yumrutaş Ö, et al. *J Surg Res.*, 2019; **233:**284-296.